

# Comparison of Oxidation Resistance of UHMWPE and POM in H<sub>2</sub>O<sub>2</sub> Solution from ReaxFF Reactive Molecular Dynamics Simulations

Wu Chen,<sup>†,‡</sup> Hai-tao Duan,<sup>†,‡</sup> Meng Hua,<sup>§</sup> Ka-li Gu,<sup>†,‡</sup> Hong-fei Shang,<sup>||</sup> and Jian Li\*,<sup>†,‡</sup>

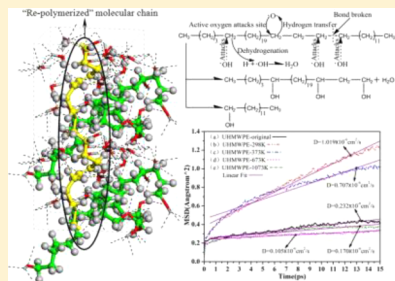
<sup>†</sup>R&D Center, Wuhan Research Institute of Materials Protection, 126 Bao Feng Erlu, Wuhan, Hubei 430030, China

<sup>‡</sup>Hubei Key Laboratory of Materials Surface Protection Technology, 126 Bao Feng Erlu, Wuhan, Hubei 430030, China

<sup>§</sup>MBE Department, City University of Hong Kong, 83 Tat Chee Avenue, Kowloon 999077, Hong Kong

<sup>||</sup>State Key Laboratory of Tribology, 9003 Building, Tsinghua University, Haidian District, Beijing 100084, China

**ABSTRACT:** The oxidation mechanism of ultra-high-molecular-weight polyethylene (UHMWPE) and polyoxymethylene (POM) in hydrogen peroxide solution was investigated by molecular dynamics (MD) simulations via reactive force field (ReaxFF) method. MD results from ReaxFF suggested that UHMWPE provided better antioxidation activity at high temperature ( $>373$  K) than its POM counterpart in the same concentration of hydrogen peroxide solution. Furthermore, POM was relatively more susceptible to erosion and swelling because of the infiltration of H<sub>2</sub>O<sub>2</sub> solution. Calculations of the diffusion coefficient at different temperatures permit further understanding of the chemical phenomena involved in the level of oxidation in the course of MD simulations. Results of the simulations are generally consistent with the previous experimental available in literature. The simulations also provide new insights into understanding the mechanism resulting oxidation products among the interested polymers.



## 1. INTRODUCTION

Many excellent properties such as good impact strength, aging resistance, and corrosion resistance of engineering plastics like ultra-high-molecular-weight polyethylene (UHMWPE) and polyoxymethylene (POM) increasingly facilitate these plastics to displace metals effectively in many engineering fields.<sup>1,2</sup> Although oxidation is inherently taking place in these components, investigation of the oxidation mechanism of these materials, which are used in some severe oxidizing environment, typically as bearings of turbo-pump, valves, and dynamic seals in liquid rocket,<sup>3,4</sup> still mostly relies on traditional experimental methods.<sup>5–7</sup> Wang et al.<sup>5</sup> studied tribological properties of UHMWPE under different concentration of hydrogen peroxide solutions and found the increase in friction coefficient with the increase in H<sub>2</sub>O<sub>2</sub> concentration. The finding suggests that strong oxidant tends to give negative impact on tribological behavior of UHMWPE. Rocha et al. investigated and characterized the accelerated degradation of UHMWPE under exposure to an aggressive hydrogen peroxide medium through the use of first-order kinetics and infrared spectroscopy.<sup>6,7</sup> Their results suggested FTIR spectroscopy to be a proven and important tool for evaluating UHMWPE degradation, which is a major species directly associated with oxidation reactions. However, the mechanism involved in the oxidation of UHMWPE is so far largely unknown, and consequently in-depth investigation in molecular transport and other microstructure changes during the oxidation process is still awaiting further exploration.

Molecular dynamics (MD) simulation is one of the important tools for studying molecular systems at an atomic level. It involves first establishing an energy expression and defining an optimized structure (if necessary) for the system of interest. It is

then followed by a series of dynamics simulations to calculate the molecular motion using the appropriately modified classical equations. The MD simulation facilitates a series of important data such as molecular configuration, atomic velocities, and some fundamental physical parameters to be obtained. Results suggest that the MD simulation is an effective research method for deeper understanding of the process and mechanism of the relevant chemical reaction. With the unremitting efforts of theoretical computational scientists in the past few years, a number of modified force fields have been developed through adequate data, which were obtained from the integration of quantum calculations and experimental study for chemical reactions of multiatom systems, for example, the developer of a reactive force field (ReaxFF).<sup>14</sup> The reliability of these force fields has been proven by much research published in literature.<sup>8–13,15–17</sup>

This paper uses the (ReaxFF)<sup>18</sup> MD to calculate the reaction processes of UHMWPE and POM in hydrogen peroxide solution at a series of temperatures (298, 373, 673, and 1073 K) with simulation time of 1000 ps (1000 ps = 1 ns), respectively. Results of the simulation provide a theoretical basis for relevant experiment phenomena and shed light for generating new research idea and for understanding the engineering plastics oxidation mechanism.

## 2. COMPUTATION METHODS

**2.1. Molecular Dynamics Theory.** The MD method calculates atomic trajectories by integrating numerically the modified classical equations of motion (eqs 1 and 2). These

Received: June 11, 2014

Revised: July 31, 2014

Published: August 18, 2014

equations have been appropriately modified so as to deal with the effects of temperature and pressure on the system adequately.

The MD of an atom  $i$  can, in a simplest form, be expressed by the most familiar Newton's equation of motion:

$$\mathbf{F}_i = m_i \mathbf{a}_i \quad (1)$$

where  $\mathbf{F}_i$  is the force,  $m_i$  is the mass, and  $\mathbf{a}_i$  is the acceleration of the atom  $i$ . Furthermore, the force on the atom  $i$  can be computed directly from the derivative with respect to the coordinate  $\mathbf{r}_i$  of its potential energy  $V_i$ :

$$-\frac{\partial V_i}{\partial \mathbf{r}_i} = m_i \frac{\partial^2 \mathbf{r}_i}{\partial t^2} \quad (2)$$

where  $t$  is the time at which the MD simulation is interested and conducted. The use of Verlet algorithm,<sup>19</sup> which is widely used in MD simulation, allows the equations of motion and velocity to be written as eqs 3–5.

$$\mathbf{r}(t + \Delta t) = \mathbf{r}(t) + \Delta t \mathbf{v}(t) + \frac{\Delta t^2 \mathbf{a}(t)}{2} \quad (3)$$

$$\mathbf{a}(t + \Delta t) = \frac{\mathbf{f}(t + \Delta t)}{m} \quad (4)$$

$$\mathbf{v}(t + \Delta t) = \mathbf{v}(t) + \frac{1}{2} \Delta t [\mathbf{a}(t) + \mathbf{a}(t + \Delta t)] \quad (5)$$

where  $\mathbf{r}(t)$  is the position,  $\mathbf{v}(t)$  is the velocity,  $\mathbf{a}(t)$  is the acceleration at time  $t$ , and  $\Delta t$  is the integral time step.

**2.2. Simulation Procedures.** The simulations were performed with molecular model of single-chain terminated with H atoms and having 20 monomers for both UHMWPE and POM, as shown in Figure 1a,b, respectively.



Figure 1. Monomers for both UHMWPE and POM.

The interactions between atoms both in the chain(s) and in the bulk polymer were taken into account by suitably imposing 3-D periodic boundary conditions. The simulated initial structures of polymer were equilibrated by the “annealing dynamics” with constant pressure and constant temperature (NPT), which is a

simulation technique for obtaining a global minimum energy of a system.<sup>20</sup> The technique involves the use of the polymer-consistent force field (PCFF)<sup>21</sup> in the “annealing dynamics” process. The range of “annealing” temperature cycle was within 298 to 600 K with a variance to be controlled to  $\pm 10$  K by suitably velocity scaling. The simulation used (i) an atom-based summation method<sup>22</sup> to calculate the van der Waals interactions with a cutoff distance of 16.5 Å and (ii) Ewald method<sup>23</sup> to calculate the electrostatic (Coulombic) interactions between atoms. The packing of optimized  $\text{H}_2\text{O}_2$  and  $\text{H}_2\text{O}$  molecular within the “annealed” structure was built by a mole ratio 5:1 (with concentration of hydrogen peroxide solution of 90%) at the appropriate density 1.39 g/mL. The thermal motion of individual atoms was initiated by randomly selecting a 3-D velocity from the Maxwell–Boltzmann distribution. Figure 2 shows the initial structures of the atoms and bonds in UHMWPE and POM with 9.89 and 9.81 Å periodic cube, respectively, as ball-and-stick model. As seen in Figure 2, the initial structural models consist of (i) the molecules of  $\text{H}_2\text{O}_2$  and  $\text{H}_2\text{O}$  molecules that are shown in stick model, (ii) the carbon atoms shown in green, (iii) oxygen shown in red, and (iv) hydrogen shown in gray.

The simulations of oxidative reaction were carried out in two stages: (i) the simulation time to be first taken as 10 ps so as to equilibrate the kinetic and potential energy distributions prior to the production phase and (ii) the simulations of reactive MD at constant volume and constant temperature (NVT) to be then undertaken by first using the potential and velocity distribution obtained from the corresponding equilibration stage (i). The Berendsen method<sup>24</sup> was used to introduce a more gentle exchange of thermal energy between the system and a heat bath with a decay constant 0.1 ps. The variation of potential and kinetic energy during production dynamics was calculated by ReaxFF, in which the duration of reactive MD was taken as 1000 ps with time of individual integral dynamics steps to be 0.2 fs (1 ps = 1000 fs).

### 3. REACTIVE MD RESULTS AND DISCUSSION

Figure 3 is the MD results for the oxidative reaction of UHMWPE simulated under four different temperatures. Simulations with duration of 1000 ps at 298 K (Figure 3a) showed that: (i) One hydrogen atom, which contacted with the carbon atom in UHMWPE molecule, was replaced by hydroxyl radical, and it left before the hydroxyl attacks the carbon. (ii) One carbon site was attacked by active oxygen, which resulted in a

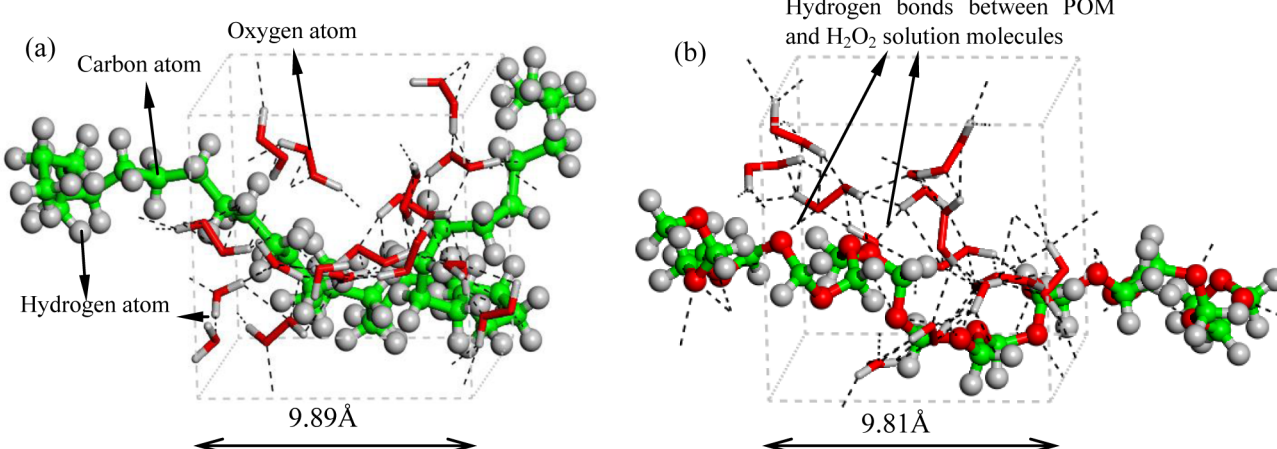


Figure 2. Model of the initial molecular structures of UHMWPE and POM, respectively, with 90%  $\text{H}_2\text{O}_2$  solutions: (a) UHMWPE + 90%  $\text{H}_2\text{O}_2$  solution and (b) POM + 90%  $\text{H}_2\text{O}_2$  solutions.

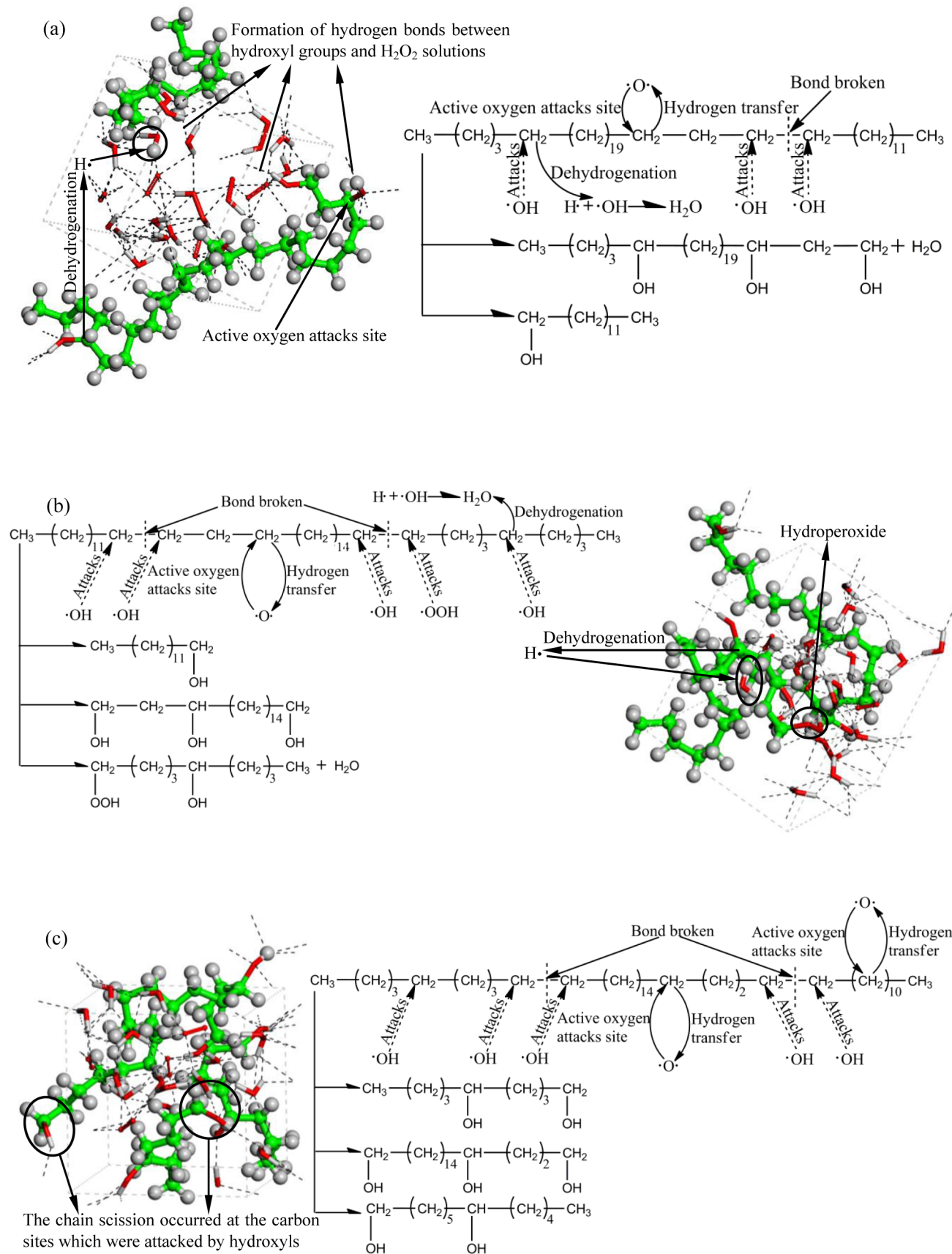
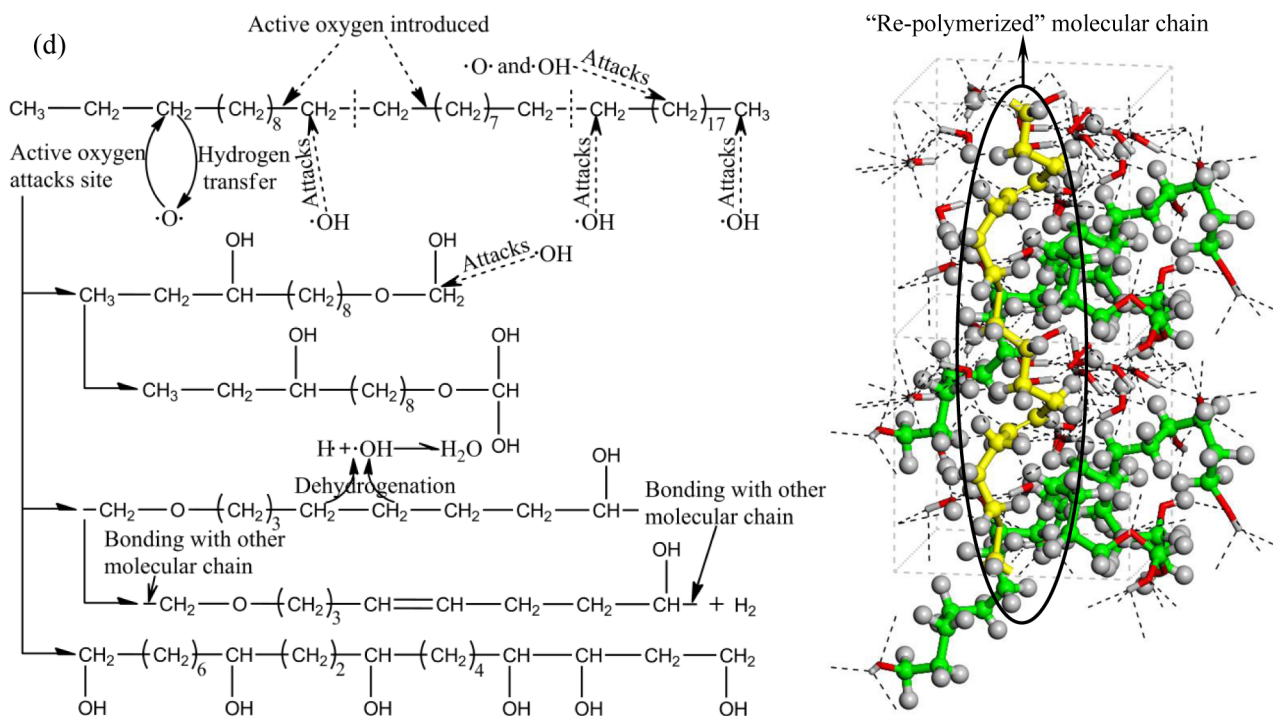


Figure 3. continued



**Figure 3.** MD results of UHMWPE in the solution with 90% concentration of  $H_2O_2$  at different temperatures contain distribution of UHMWPE oxidation products and mechanism of oxidative reaction: (a) after 298 K MD; (b) after 373 K MD; (c) after 673 K MD; and (d) after 1073 K MD.

formation of hydroxyl group. The active oxygen ion  $\cdot\text{O}\cdot$  came from the decomposition of unstable structure of peroxide radical  $\cdot\text{OO}\cdot$  or hydroperoxide radical  $\cdot\text{OOH}$ . These radicals as well as hydroxyl  $\cdot\text{OH}$  and hydrogen  $\text{H}\cdot$  radicals generally exist in hydrogen peroxide solution; they are likely to spontaneously decompose under the light irradiation or high temperature.

(iii) A chain scission occurred between two carbon sites of introduced hydroxyl. The hydroxyl radicals generally existed in  $\text{H}_2\text{O}_2$  solutions. Aiming at revealing further reactions, a higher temperature simulation of 1000 ps at 373 (Figure 3b) and 673 K (Figure 3c), respectively, was carried out. Simulation illustrated that one more chain scission at the carbon sites to be attacked by hydroxyls occurred at the two higher temperatures (cf. Figures 3a–c). Such result suggested: (i) the weakening of the stability of C–C single bond by the introduction of hydroxyl group<sup>6</sup> and (ii) the increasing of temperature raising up the number of hydroxyl groups. The instability of hydroperoxide, as observed in the still frame of molecular structure (Figure 3b), tends to form to be further oxidized to carboxyl or decompose spontaneously. Aiming at better understanding the process of oxidation, MD simulation with duration of 1000 ps and temperature of 1073 K was performed. The result of the simulation (Figure 3d) suggested that the occurrence of dehydrogenation and the attachment of activated oxygen in  $\text{H}_2\text{O}_2$  solutions promoted the formation of C=C double bond and R-O-R' ethers. It also revealed that a significant increment in the number of hydroxyl groups took place without any additional chain scission to be seen. Furthermore, the formation of other degraded products like  $\text{H}_2$  and  $\text{H}_2\text{O}$  was also observed. Comparing the original UHMWPE structure (Figure 2a) to the structure resulted from the MD simulation with 1073 K–1000 ps (Figure 3d); it showed that the original organized structure of polymer chain was severely randomized under the MD-simulated conditions. Because of the nature of (i) forming intermolecular

hydrogen bonds and (ii) bonding between chain fragment of the terminating carbon atoms and other products originally belonging to adjacent cells, a process similar to “re-polymerization” (Note: The two periodic Amorphous cells marked with yellow in Figure 3d are the “re-polymerized” backbones), the presence of cross-linking chains is usually expected in some polymers. In general, the highly dense and linear UHMWPE network restricts oxygen and oxidizing radicals to diffuse through, which would most likely be the mechanism to cause the sharp drop of oxidation kinetic rate. Our simulation results seem to be consistent with the available literature.<sup>6,7,25–31</sup>

MD results of POM in hydrogen peroxide solutions are illustrated in Figure 4. Results of POM simulated with 1000 ps MD at 298 and 373 K showed the absence of oxidative degradation at lower simulation temperatures, suggesting better oxidative stability of POM compared with that of UHMWPE in the initial stage of oxidative reaction. Aiming at revealing more chain fragmentations, “depolymerization” simulation with 1000 ps at a higher temperature of 673 K (Figure 4a) was carried out. Similar to the MD result of UHMWPE at 298 K (Figure 2a), the attack of active radical to POM chain tended to activate chain reactions and subsequently decomposed the model compounds.

It is noteworthy that the oxidation of POM by introduction of hydroxyl resulted in the formation of intramolecular hydrogen bonds between functional groups and oxygen atoms existing in the POM backbone. The stability of C–O bonds in POM backbone was subjected to adverse effect due to the increase in the number of intermolecular and intramolecular hydrogen bonds and subsequently accelerated the oxidative degradation of POM. At a high temperature of 1073 K, the rate of decomposition was further enhanced (Figure 4b). The scission and termination of C–O bonds led to the formation of branches and instable structures of carbon with many hydroxyls, which

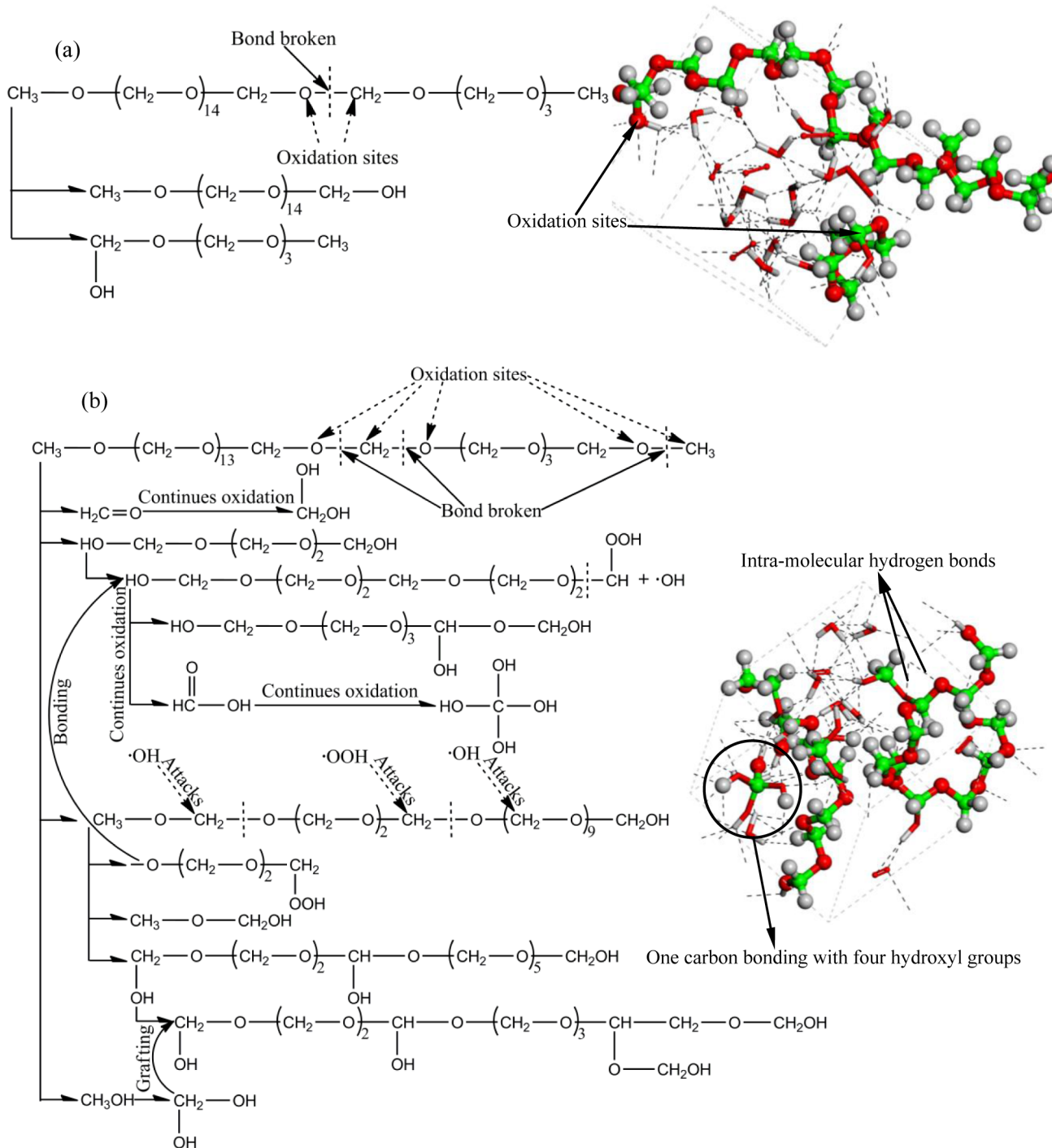


**Figure 4.** MD results of POM in the solution with 90% concentration of  $\text{H}_2\text{O}_2$  at different temperatures contain distribution of POM oxidation products and mechanism of oxidative reaction: (a) after 673 K MD and (b) after 1073 K MD.

further promulgated the formation of small molecular fragments. Most reactions within the hydroxyl groups resulted in the suitable bonding with a carbon atom, which subsequently spontaneously transformed the hydroxyl groups to  $\text{H}_2\text{O}$ ,  $\text{C}=\text{O}$  bonds, or carboxyls, and so on. These reactions might lead to decreasing the degree of chain cross-linking in POM. The molecules in  $\text{H}_2\text{O}_2$  solutions gained higher mobility to infiltrate in lower degree of chain cross-linking, which resulted in interior swelling and erosion. The aforementioned observations and analyses show the quality deterioration of POM matrix materials in hydrogen peroxide solution, and POM is unsuitable to be

used in some environments and conditions involved with severe oxidizing.

#### 4. DIFFUSIVITY OF $\text{H}_2\text{O}_2$ SOLUTIONS

The capacity of the polymers to constrain small molecules can be assessed by the diffusion coefficient of small molecules in polymers. Calculation of the changes of diffusion coefficient of  $\text{H}_2\text{O}_2$  solution in polymers before and after MD simulations, respectively, at different temperatures facilitates the understanding of the mechanism of (i) reaction and (ii) causing the variation of the oxidation rate.

The diffusion coefficient  $D$  can be expressed in terms of the increase in mean-square displacement (MSD) of atoms with time as eq 6 later:<sup>32</sup>

$$D = \frac{1}{6N} \lim_{t \rightarrow \infty} \frac{d}{dt} \sum_{i=1}^N \langle [r_i(t) - r_i(0)]^2 \rangle \quad (6)$$

where  $N$  is the number of diffusive atoms (which belongs to all small molecules, free radicals and active oxygen that generally existed in  $H_2O_2$  solution) in the system;  $r_i(t)$  is the position vector of  $i$ th particle at time  $t$ ; and  $r_i(0)$  is the position vector of  $i$ th particle at time origin. The right-hand side expression is the mean-square displacement and is taken as an averaging operator  $\langle \bullet \rangle$ .

When the time  $t$  is sufficiently large, the diffusion coefficient for any of the individual diffusive atoms is simply expressed as

$$D = \frac{\langle [r(t) - r(0)]^2 \rangle}{6t} = \frac{S_{MSD}}{6t} \quad (7)$$

where  $S_{MSD}$  is a curve fitting to all MSD data versus time, as seen in Figures 5 and 6.

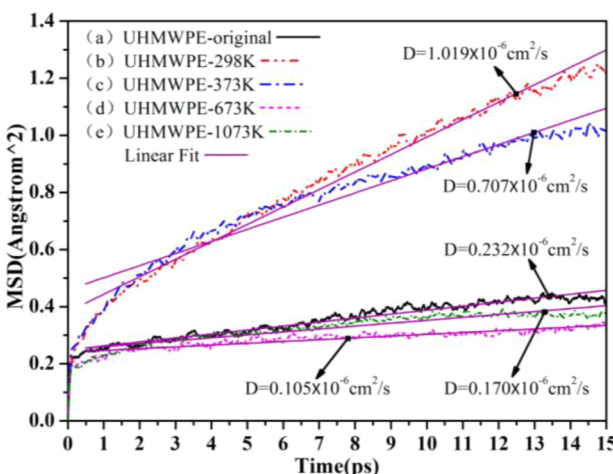


**Figure 5.**  $S_{MSD}$  curve and diffusion coefficient  $D$  of  $H_2O_2$  solution in UHMWPE molecular chains after MD simulation at different temperatures: (a) model of original UHMWPE in  $H_2O_2$  solution; (b) after 1000 ps–298 K MD; (c) after 1000 ps–373 K MD; (d) after 1000 ps–673 K MD; (e) and after 1000 ps–1073 K MD.

The diffusion coefficient in this study was determined by fitting the data in the diffusive part of  $S_{MSD}$  with a linear function  $y = kx + b$  (see: purple section of the curves in Figure 5 and 6), which gives a slope  $k$  in units of  $\text{Å}^2/\text{ps}$ . According to the definition in eq 7, subsequently, the diffusion coefficient  $D$ , according to the definition in eq 7 can be simplified as

$$D = \frac{k}{6} \quad (8)$$

Hence, the diffusion coefficient  $D$  (with unit converted to  $\text{cm}^2/\text{s}$ ) can be obtained from solving of the function  $S_{MSD}$ . The diffusion coefficient  $D$  of (i) the original model (Figure 1) and (ii) the final structures after reactive molecular dynamics simulations with duration of 50 ps for a series of temperatures was calculated. The calculation was also undertaken at constant volume and constant energy (NVE). Although NVE dynamics does not vary the thermodynamic state of a system, the thermo-stating condition selected for the simulation significantly alters the final structure and subsequently the diffusion coefficient.

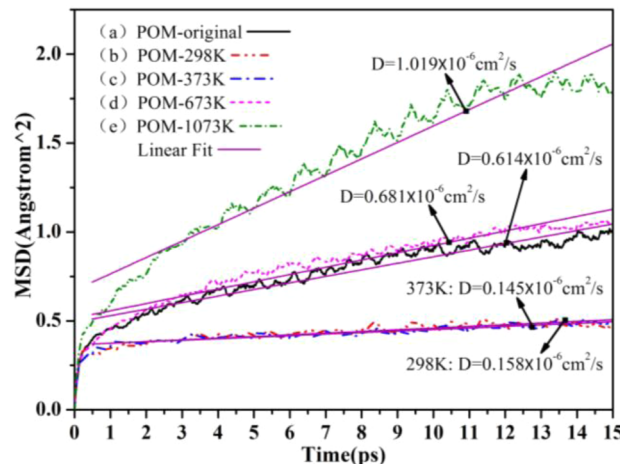


**Figure 6.**  $S_{MSD}$  curve and diffusion coefficient  $D$  of  $H_2O_2$  solution in POM molecular chains after MD simulation at different temperatures: (a) model of original POM in  $H_2O_2$  solution; (b) after 1000 ps–298 K MD; (c) after 1000 ps–373 K MD; (d) after 1000 ps–673 K MD; and (e) after 1000 ps–1073 K MD.

The full information like temperature, energies, velocities, cell parameters, and so on was instantaneously recorded for the calculation of mean square displacement. The curve of  $S_{MSD}$  and the diffusion coefficient  $D$  of  $H_2O_2$  solution in UHMWPE and POM molecular chains are, respectively, displayed in Figures 5 and 6.

Diffusion coefficient  $D$  used for determining the capacity of polymers in constraining small molecules. In general, smaller  $D$  means higher capacity of polymer to constrain  $H_2O_2$  solution. Once the surface of polymer was oxidized by  $H_2O_2$  solution in real system, the greater diffusion coefficient indicated that the  $H_2O_2$  solutions are relatively easier to infiltrate into interior of polymer and subsequently lead to interior erosion or swelling, it is negative to oxidation resistance of polymers. We calculate the MSD by averaging the MSDs calculated for each of the three separate MD runs. Figure 7 displays the variation of diffusion

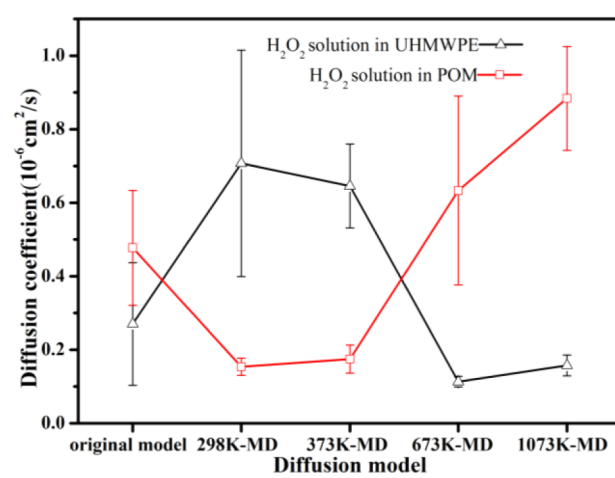


**Figure 7.** Variation of diffusion coefficient of  $H_2O_2$  solution within polymer molecular chains.

coefficients of  $H_2O_2$  solution in UHMWPE and POM molecular chains. It was observed that the diffusion coefficients of  $H_2O_2$  solution in UHMWPE increased with the increase in simulation temperatures at reactive MD simulations temperatures below 373 K. However, it showed a decreasing trend once the

temperatures for the reactive MD simulations were beyond 373 K. For example, the diffusion coefficients for the 1073 K MD simulations were lower than those for their original counterpart, indicating the enhancement of the capacity of UHMWPE to constrain  $H_2O_2$  solution with higher reactivity condition. The result allows the speculation that the interior of UHMWPE materials is likely protected by the oxide layer in the real system, and the oxidative reaction would be terminated by the formation of oxide layer. Presumably these occurrences of such protection may mainly be due to the increasing of the cross-linking and the number of intermolecular hydrogen bonds in UHMWPE molecular chains. The aforementioned analytical results of these oxidation behaviors by the diffusion coefficient were consistent with other experiment available in the literature.<sup>27,30,31,33–35</sup>

The variation of diffusion coefficient of  $H_2O_2$  solution, as predicted in POM model, showed a decreasing trend with the increase in simulation temperatures when the temperatures for the reactive MD simulations were at and below 373 K. However, their counterparts gave increasing trend instead when the reactive MD simulations temperatures were beyond 373 K; the value became the greatest with the 1073 K MD case. This suggests that the capacity of POM to constrain  $H_2O_2$  solution is enhanced in the initial reaction stage and subsequently diminished with higher thermal reactivity. As a result the molecules in  $H_2O_2$  solutions are relatively easier to infiltrate and to swell within POM molecular chains, which susceptibly leads to interior erosion.

The easier infiltration of  $H_2O_2$  solutions is probably due to weakening of the bond energy of C–O in POM molecules as the effect of introduction of hydroxyl, which subsequently creates “inter-molecular gap” to promote solution molecules infiltrating into POM surface because of the formation of small molecular fragments destroying POM molecular chains cross-linking. Analysis of the diffusion coefficient with the POM model suggests the steep rise oxidation rate with increasing of MD simulation temperatures. Such increase expedites the small molecules to become oxidative products.

## 5. CONCLUSIONS

Analysis of the results of MD simulations facilitates the following conclusions to be made:

(1) Dehydrogenation, introduction of hydroxyl, and dissociation of C–C bond are basically the dominant factors resulting in the oxidative reaction of UHMWPE in  $H_2O_2$  solution. Although alcohols are the main products with a high-molecular-weight fraction, our simulations have illustrated the existence of other small molecular products like  $H_2O$  and  $H_2$ . However, there is not any other small molecular degradation product to be observed among the oxidation products produced. The capacity of UHMWPE to constrain  $H_2O_2$  solution has been found to be suitably enhanced with higher thermal reactivity, and it is observed that there is not any significant increase in the oxidation rate of UHMWPE.

(2) Introduction of hydroxyl and breaking of C–O bond are the dominant factors resulting in the oxidative reaction of POM in  $H_2O_2$  solution. Alcohols with branch of high-molecular-weight fraction and small molecular degradation products are the main products in serious oxidative degradation. The capacity of POM to constrain  $H_2O_2$  solution becomes lower with higher thermal reactivity, which subsequently significantly increases the oxidation rate of POM. Moreover, it leads POM to be susceptible to erosion and swelling. Hence, POM is not suitable to be used in severe oxidizing environment.

(3) Most of simulation results seem to correlate well with the experimental results, with respect to oxidation products, in available literature. The simulation provides the theoretical basis for further investigation of oxidation mechanism of these thermoplastics in severe oxidizing environment.

## AUTHOR INFORMATION

### Corresponding Author

\*E-mail: lijianwuhan@163.net.

### Notes

The authors declare no competing financial interest.

## ACKNOWLEDGMENTS

We are grateful for the financial support of the National Natural Science Foundation of China (No. 51275361), the National Scientific and Technical Project of China (No. 2013CB632303), and the Tribology Science Fund of State Key Laboratory of Tribology, Tsinghua University (SKLTKF13A07), China.

## REFERENCES

- Lai, H. Plastic Engineering Materials Applied in Automobile Manufacturing. In *Proceedings of the 9th International Symposium on Linear Drives for Industry Applications*, Liu, X. Z., Ye, Y. Y., Eds.; Springer: Berlin, 2014; Vol. 1, pp 141–145.
- Wang, X. M.; Yang, C.; Li, B. Z. Advance in the Engineering Plastics Application of China in 2012. *Eng. Plast. Appl.* 2013, 41 (6), 93–102.
- Yu, D. Y.; Xue, Q. J. Frontiers for Space Tribology Investigation. *Tribology* 1997, 17 (4), 380–384.
- Krishnan, S.; Ahn, S. H.; Lee, C. W. Design and development of a hydrogen-peroxide rocket-engine facility. *J. Mekanikal* 2010, 30, 24–36.
- Wang, J. P.; Duan, H. T.; Wang, D.; Tu, J. S.; Wu, Y. M.; Li, J. Tribological Properties of Ultrahigh Molecular Weight Polyethylene in Hydrogen Peroxide Solution. *Mater. Mech. Eng.* 2013, 37 (6), 48–51.
- Rocha, M. F.; Mansur, A. A. P.; Mansur, H. S. Characterization and accelerated ageing of UHMWPE used in orthopedic prosthesis by peroxide. *Mater.* 2009, 2 (2), 562–576.
- Rocha, M. F.; Mansur, A. A. P.; Mansur, H. S. FTIR Investigation of UHMWPE Oxidation Submitted to Accelerated Aging Procedure. *Macromol. Symp.* 2010, 296 (1), 487–492.
- Nyden, M. R.; Stolarov, S. I.; Westmoreland, P. R. Applications of reactive molecular dynamics to the study of the thermal decomposition of polymers and nanoscale structures. *Mater. Sci. Eng., A* 2004, 365, 114–122.
- Stolarov, S. I.; Lyon, R. E.; Nyden, M. R. A reactive molecular dynamics model of thermal decomposition in polymers: II. Polyisobutylene. *Polymer* 2004, 45, 8613–8621.
- Diao, Z.; Zhao, Y.; Chen, B.; Duan, C.; Song, S. ReaxFF reactive force field for molecular dynamics simulations of epoxy resin thermal decomposition with model compound. *J. Anal. Appl. Pyrolysis* 2013, 104, 618–624.
- Salmon, E.; van Duin, A. C.; Lorant, F.; Marquaire, P. M.; Goddard, W. A., III. Thermal decomposition process in algaenan of *Botryococcus braunii* race L. Part 2: Molecular dynamics simulations using the ReaxFF reactive force field. *Org. Geochem.* 2009, 40 (3), 416–427.
- Mueller, J. E.; van Duin, A. C.; Goddard, W. A. Application of the ReaxFF reactive force field to reactive dynamics of hydrocarbon chemisorption and decomposition. *J. Phys. Chem. C* 2010, 114 (12), 5675–5685.
- Chen, B.; Wei, X. Y.; Yang, Z. S.; Liu, C.; Fan, X.; Qing, Y.; Zong, Z. M. ReaxFF reactive force field for molecular dynamics simulations of lignite depolymerization in supercritical methanol with lignite-related model compounds. *Energy Fuels* 2012, 26 (2), 984–989.
- Salmon, E.; van Duin, A. C.; Lorant, F.; Marquaire, P. M.; Goddard, W. A., III. Early maturation processes in coal. Part 2: Reactive dynamics simulations using the ReaxFF reactive force field on Morwell Brown coal structures. *Org. Geochem.* 2009, 40 (12), 1195–1209.

- (15) Nielson, K. D.; van Duin, A. C.; Oxgaard, J.; Deng, W. Q.; Goddard, W. A. Development of the ReaxFF reactive force field for describing transition metal catalyzed reactions, with application to the initial stages of the catalytic formation of carbon nanotubes. *J. Phys. Chem. A* **2005**, *109* (3), 493–499.
- (16) Mueller, J. E.; van Duin, A. C.; Goddard III, W. A. Development and validation of ReaxFF reactive force field for hydrocarbon chemistry catalyzed by nickel. *J. Phys. Chem. C* **2010**, *114* (11), 4939–4949.
- (17) Leininger, J.; Minot, C.; Lorant, F. Two theoretical simulations of hydrocarbons thermal cracking: Reactive force field and density functional calculations. *J. Mol. Struct.: THEOCHEM* **2008**, *852* (1), 62–70.
- (18) Van Duin, A. C.; Dasgupta, S.; Lorant, F.; Goddard, W. A. ReaxFF: a reactive force field for hydrocarbons. *J. Phys. Chem. A* **2001**, *105* (41), 9396–9409.
- (19) Martys, N. S.; Mountain, R. D. Velocity Verlet algorithm for dissipative-particle-dynamics-based models of suspensions. *Phys. Rev. E* **1999**, *59* (3), 3733.
- (20) Kirkpatrick, S.; Vecchi, M. P. Optimization by simulated annealing. *Science* **1983**, *220* (4598), 671–680.
- (21) Sun, H. Ab initio calculations and force field development for computer simulation of polysilanes. *Macromolecules* **1995**, *28* (3), 701–712.
- (22) Kantola, A.; Villar, H. O.; Loew, G. H. Atom based parametrization for a conformationally dependent hydrophobic index. *J. Comput. Chem.* **1991**, *12* (6), 681–689.
- (23) Ewald, P. P. Ewald summation. *Ann. Phys.* **1921**, *369*, 253.
- (24) Berendsen, H. J. C.; Postma, J. P. M.; van Gunsteren, W. F.; DiNola, A.; Haak, J. R. Molecular dynamics with coupling to an external bath. *J. Chem. Phys.* **1984**, *81*, 3684–3690.
- (25) Gugumus, F. Thermooxidative degradation of polyolefins in the solid state: Part 1. Experimental kinetics of functional group formation. *Polym. Degrad. Stab.* **1996**, *52* (2), 131–144.
- (26) Kurtz, S. M.; Pruitt, L.; Jewett, C. W.; Paul Crawford, R.; Crane, D. J.; Edidin, A. A. The yielding, plastic flow, and fracture behavior of ultra-high molecular weight polyethylene used in total joint replacements. *Biomaterials* **1998**, *19* (21), 1998–2003.
- (27) Bracco, P.; Brunella, V.; Zanetti, M.; Luda, M. P.; Costa, L. Stabilisation of ultra-high molecular weight polyethylene with vitamin E. *Polym. Degrad. Stab.* **2007**, *92* (12), 2155–2162.
- (28) Costa, L.; Luda, M. P.; Trossarelli, L.; Brach del Prever, E. M.; Crova, M.; Gallinaro, P. Oxidation in orthopedic UHMWPE sterilized by gamma-radiation and ethylene oxide. *Biomaterials* **1998**, *19* (7–9), 659–668.
- (29) Rimnac, C. M.; Kurtz, S. M. Ionizing radiation and orthopaedic prostheses. *Nucl. Instrum. Meth. B* **2005**, *236* (1), 30–37.
- (30) Reggiani, M.; Tinti, A.; Visentin, M.; Stea, S.; Erani, P.; Fagnano, C. Vibrational spectroscopy study of the oxidation of Hylamer UHMWPE explanted acetabular cups sterilized differently. *J. Mol. Struct.* **2007**, *834*, 129–135.
- (31) Taddei, P.; Affatato, S.; Fagnano, C.; Bordini, B.; Tinti, A.; Toni, A. Vibrational spectroscopy of ultra-high molecular weight polyethylene hip prostheses: influence of the sterilization method on crystallinity and surface oxidation. *J. Mol. Struct.* **2002**, *613* (1), 121–129.
- (32) Jost, S.; Biswas, P.; Schüring, A.; Kärger, J.; Bopp, P. A.; Haberlandt, R.; Fritzsche, S. Structure and self-diffusion of water molecules in chabazite: A molecular dynamics study. *J. Phys. Chem. C* **2007**, *111* (40), 14707–14712.
- (33) Lee, A. W.; Santerre, J. P.; Boynton, E. Analysis of released products from oxidized ultra-high molecular weight polyethylene incubated with hydrogen peroxide and salt solutions. *Biomaterials* **2000**, *21* (8), 851–861.
- (34) Medel, F. J.; Garcia-Alvarez, F.; Gomez-Barrena, E.; Puertolas, J. A. Microstructure changes of extruded ultra high molecular weight polyethylene after gamma irradiation and shelf-aging. *Polym. Degrad. Stab.* **2005**, *88* (3), 435–443.
- (35) Toohey, K. S.; Blanchet, T. A.; Heckelman, D. D. Effect of accelerated aging conditions on resultant depth-dependent oxidation and wear resistance of UHMWPE joint replacement bearing materials. *Wear* **2003**, *255* (7), 1076–1084.